Propagating surface plasmon polaritons in graphene under applied uniform strain

A. Galeana and G. González de la Cruz

Departamento de Física, CINVESTAV-IPN,
apartado postal 14-740 CDMX, México.
e-mail: luis.galeana@cinvestav.mx; bato@fis.cinvestav.mx

Received 12 July 2023; accepted 18 November 2023

In this work, we theoretically investigate the propagation length of plasmon waves in graphene layer under uniform strain surrounded by two dielectric media of dielectric constants ε_1 and ε_2, respectively. The plasmon losses (plasmon damping), plasmon propagation length and the penetration depth of the electric field associates with the charge fluctuations can be controlled by varying the direction and the strength of the applied strain and the direction of the plasmon wave propagation with respect to the direction of the applied strain. Because strain induces anisotropy in graphene optical conductivity, the strain-dependent orientation plays an important role to manipulate the direction and variations of the graphene plasmon energy, which may be useful to tune graphene properties in plasmonic devices to enhance light-matter interaction.

Keywords: Graphene; strain; optical conductivity; plasmons.

DOI: https://doi.org/10.31349/RevMexFis.70.020502

1. Introduction

Surface-plasmons (SPs) are electromagnetic excitations waves coupled with charge density oscillations (plasmons) traveling along metal-dielectric interface. The electric field associated with these oscillations decay exponentially into the dielectric environment making plasmons extremely sensitive to the refractive index of the surrounding materials. They are finding increasing applications in many research fields, reaching from biosensors for the detection of biomolecules to plasmonics [1–3].

One of the main obstacles in developing plasmonic applications in metallic devices is its surface easily oxides, the Ohmic heat effect in metals results in a large loss of plasmons, poor tunability for surface plasmons and, consequently, a limited propagation length for the surface plasmons [4]. To overcome these deficiencies graphene has emerged as an alternative two-dimensional material able to extend the field for innovative plasmonic devices and possible applications in photonics, optoelectronic and sensor technologies [5–20]. However, the plasmon loses must be evaluated and minimized prior to the use of graphene as a potential alternative low lose plasmonic material.

When a graphene layer is subjected to mechanical strain, the optical response of graphene can be easily tuned by strain engineering [21, 22]. In particular, the influence of the strain on several electronic properties also produces significantly changes on the electronic polarizability and thereby collective electronic excitations associated with anisotropic optical conductivity [23–25]. Recently [26, 27] collective electronic excitations have been investigated in graphene under uniform strain. These authors showed that collective charge density excitations and optical reflectance can efficiently controlled by strain, and it is possible to overcome the mismatch between the momentum of the surface plasmon and that of incident radiation and thereby improve the light-matter interaction. Additionally, the strong anisotropy can be used to guide the plasmon modes with new properties in the field of plasmonics.

In this work, we theoretically investigate the propagation characteristics of surface plasmon in graphene under uniform strain. For this purpose, we make use of the linear response theory and the relaxation time approximation (finite τ) introduced by Mermin [28]. It has been shown that the zeros of the real dielectric function reproduce the plasmon frequency in the long wavelength approximation obtained in Ref. [26]. In addition, we have performed a numerical analysis of the penetration depth and the propagation length of surface plasmon propagation in deformed graphene as a function on the magnitude and orientation of the applied strain with respect to the plasmon propagation. Long range surface plasmons in monolayer graphene under uniform strain have been theoretically investigated in Refs. [30] these authors showed that at low photon energies, the wavelength, propagation length and penetration of the TM surface plasmon polariton increase with increasing the strain in the zigzag graphene direction.

2. Theoretical approach

In Fig. 1 is depicted the system studied in this work. A monolayer graphene is placed on a flexible substrate and the x-axis is chosen along the zigzag direction of graphene. When the system is under a uniform strain along the prescribed direction in the range of elastic deformation, the dispersion relation of the plasmon reads [26],

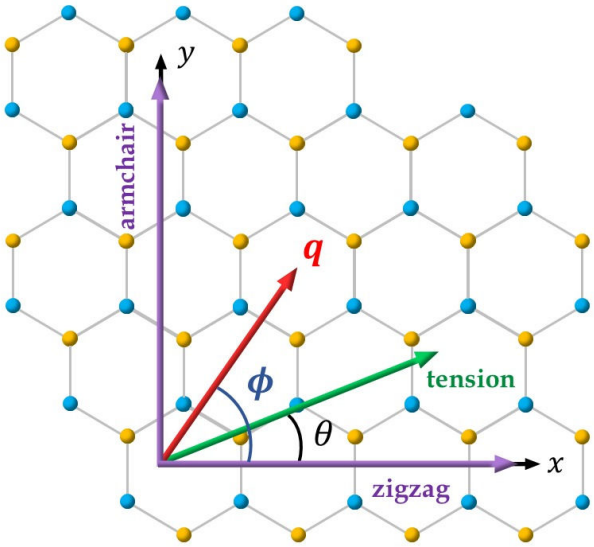

FIGURE 1. Two-dimensional graphene lattice with zigzag and armchair orientations and the applied strain (angle θ) and surface plasmon propagation (angle ϕ) directions.

$$\omega^2(\mathbf{q}) = \frac{4e^2E_f}{\varepsilon_1+\varepsilon_2}\mathbf{q}\left[1-\beta(1+\rho)\varepsilon\cos\left(2\theta-2\phi\right)\right], \quad (1)$$

where ε is the strain modulus, θ denotes the angle between the applied tension and the x-axis, and ρ being the Poisson ratio, $\beta \sim 2.37$ is the Gruneisen parameter, E_f the Fermi energy, ε_1 and ε_2 the dielectric constants surrounded the graphene layer and $\mathbf{q} = q(\cos\phi, \sin\phi)$ is the wave vector associated with the plasmon propagation induced in the strained graphene. When electron collisions by phonons, impurities (extrinsic scattering) are considered and intrinsic electron-hole excitation (Landau damping), the electron polarizability is a complex-valued function of the wavevector $\mathbf{q}$ and the frequency ω. To account for Landau damping, extrinsic scattering and conservation of local electron number, the electron polarizability should be calculated within the random-phase approximation and the relaxation-time (finite $\gamma = \tau^{-1}$) approximation introduced by Mermin, see Refs. [28–30]. Here γ^{-1} is the electron-phonon relaxation time estimate from $\gamma^{-1} = \mu E_f/ev_f^2$, $v_f{=}c/300$ is the Fermi velocity, and μ is the DC mobility of graphene (10000 cm^2/Vs) and T the temperature. Under this approach the polarizability is expressed as,

$$\Pi_\gamma(q,\omega) = \frac{\left(1+\frac{i\gamma}{\omega}\right)\Pi(q,\omega+i\gamma)}{1+\frac{i\gamma}{\omega}\frac{\Pi(q,\omega+i\gamma)}{\Pi(q,0)}}, \quad (2)$$

where $\Pi(q,\omega)$ is the electron polarizability for graphene under uniform strain and is given as [26],

$$\Pi(q,\omega) = \frac{E_f}{\pi}\frac{q^2}{\omega^2}\left(1-\frac{\omega^2}{4E_f^2}\right) \times\left[1-\beta(1+\rho)\varepsilon\cos(2\theta-2\phi)\right]. \quad (3)$$

Then, within linear response theory the dielectric function $\varepsilon(q,\omega) = 1 - V_q\Pi_\gamma(q,\omega) = 0$ can be satisfied only when the wavevector is a complex number: $q = q_1 + iq_2$, where $L_p = 1/q_2$ determines plasmon propagation length in graphene under uniform strain, physically, it represents the distance over which the electric field associated to the surface charge oscillations decays from its local maximum in the graphene supporting interface. Note that when $\gamma = 0$, the two-dimensional polarizability of graphene under uniform strain is recovered, see Ref. [26]. The solutions of the condition $\varepsilon(q,\omega) = 0$ with complex q can be separated in the real and imaginary parts in the limit small q_2/q_1 to obtain,

$$\frac{\varepsilon_1}{\sqrt{q_1^2-\frac{\varepsilon_1\omega^2}{c^2}}} + \frac{\varepsilon_2}{\sqrt{q_1^2-\frac{\varepsilon_2\omega^2}{c^2}}} - \frac{e^2}{q_1^2}\mathrm{Re}\Pi(q,\omega) = 0, \quad (4)$$

where in the nonretarded limit $\omega << c$ and in the long wavelength approximation, $q_1 \to 0$, the plasmon dispersion for graphene under uniform strain is obtained, Eq. (3), and from the imaginary part of $\varepsilon(q,\omega) = 0$ we obtain q_2 which determines the attenuation of the surface plasmon. Here $\Pi^{(1,0)}(q_1,\omega) = \partial\Pi(q_1,\omega)/\partial q_1$ and $\Pi^{(0,1)}(q_1,\omega) = \partial\Pi(q_1,\omega)/\partial\omega$ evaluated at $\omega = \omega(q)$, the plasmon frequency. As a result, the expression for q_2 given in Eq. (5) reduces to that obtained for a monolayer graphene sandwiched between dielectrics ε_1 and ε_2 for unstrained graphene *i.e.*, $\varepsilon = 0$ [29],

$$q2 = \frac{\mathrm{Im}\Pi(q_1,\omega) + \gamma\mathrm{Re}\Pi^{(0,1)(q_1,\omega)} + \frac{\gamma}{\omega}\mathrm{Re}\left[\Pi(q_1,\omega)\left(1-\frac{\Pi(q_1,\omega)}{\Pi(q_1,0)}\right)\right]}{\frac{\mathrm{Re}\Pi(q_1,\omega)}{q_1} - \mathrm{Re}\Pi^{(1,0)}(q_1,\omega)}. \quad (5)$$

As a result, the expression for q_2 given in Eq. (5) reduces to that obtained for a monolayer graphene sandwiched between dielectrics ε_1 and ε_2 for unstrained graphene *i.e.*, $\varepsilon = 0$ [29]. Another property of surface plasmons is the confinement length. The excited surface plasmon in graphene have associated evanescent fields penetrating in both dielectric mediums. They are spatially decaying fields in a direction normal to the interface between the dielectric materials. In this case, the penetration depths in the dielectric defined by

$$\delta_{1,2} = \frac{1}{\sqrt{q_1^2-(\varepsilon_{1,2}\omega^2)/c^2}}$$

at which the electric fields fall to $1/e$ of their initial magnitude.

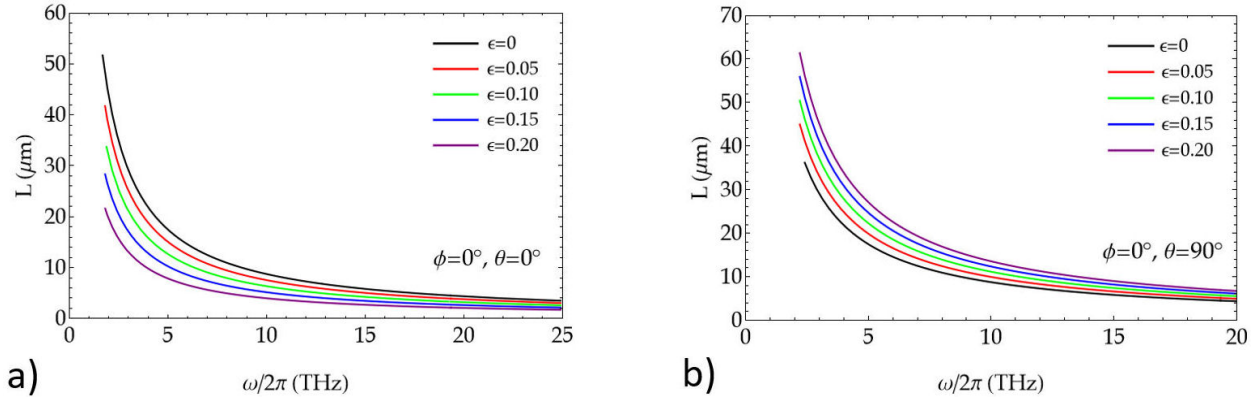

FIGURE 2. Propagation length of surface plasmon in graphene versus frequency for different applied uniform strain along the plasmon wave propagation, $\theta-\phi=0$ [Fig. 2a)] and perpendicular to the plasmon wavevector q *i.e.*, $\theta-\phi=\pi/2$ [Fig. 2b)]. Here, $E_f=0.5$ eV, $\varepsilon_1=2.25$, $\varepsilon_2=3.8$ and $\mu=10^4$ cm^2/V·s.

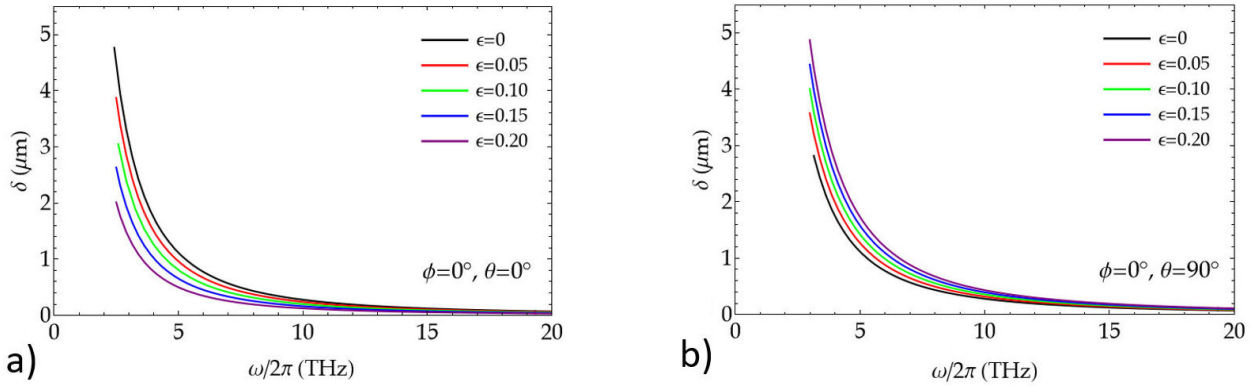

FIGURE 3. Penetration depth of surface plasmon in graphene versus frequency for different applied uniform strain along the plasmon wave propagation, $\theta-\phi=0$ [Fig. 2a)] and perpendicular to the plasmon wavevector q *i.e.*, $\theta-\phi=\pi/2$ [Fig. 2b)]. Here, $E_f=0.5$ eV, $\varepsilon_1=2.25$, $\varepsilon_2=3.8$ and $\mu=10^4$ cm^2/V·s.

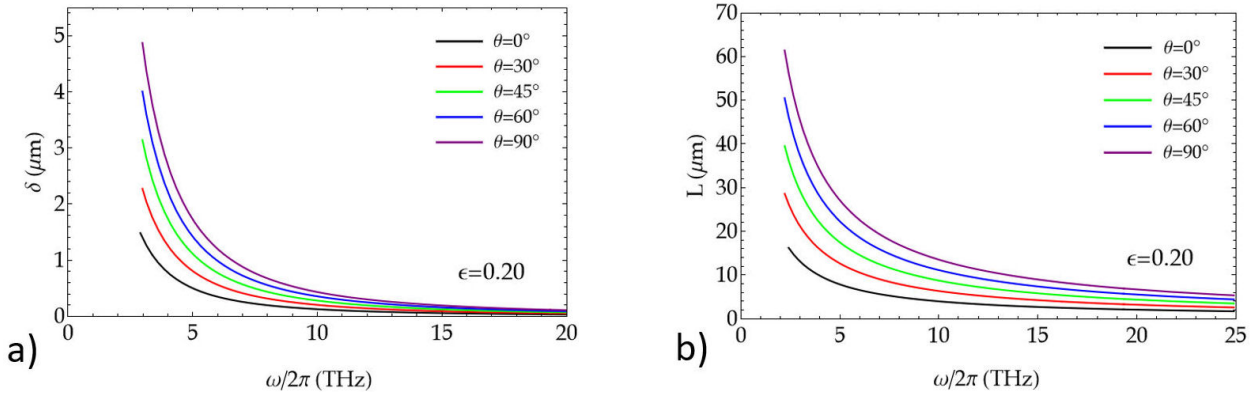

FIGURE 4. The penetration depth (a) and propagation length (b) of surface plasmon on graphene for different orientations of the applied strain and a fixed magnitude of $\varepsilon=0.2$. The other parameters are the same as in Fig. 2.

The propagation length of surface plasmons in graphene for different strength applied strain is shown in Fig. 2a) for plasmon propagation along the applied strain *i.e.*, $\theta=\phi$. It is clear from the figure that the propagation lengths decrease when the strain increase and all of them decrease with higher excitation frequency, on the other hand, when the plasmon propagates perpendicular to the applied strain ($\theta=\pi/2$, $\phi=0$) the plasmon propagation length increase with the applied strain. This shows that we can control the propagation length of surface plasmons by tunning the orientation of the applied strain respect to plasmon propagation in graphene. Also, note that the propagation length when the wavevec-

tor of the plasmon is orthogonal to strain orientation dominates for all deformation and excitation energies. According with Eq. (1), for bigger plasmon energy, plasmon propagates in graphene longer distances and this occurs when plasmon propagation is perpendicular to the direction of the applied strain.

In Fig. 3, the penetration depth of surface plasmons for different strength of the strain is plotted for plasmon propagation parallel, Fig. 3a) and perpendicular, Fig. 3b), respectively, as a function of the excitation frequency. The penetration depths of all applied strain decrease when the excitation energy is increased. It is evident from the figure that the penetration depth for parallel propagation of plasmon respect to the applied deformation decreases with the strain, Fig. 3a), while it increases when the strain increases for plasmon propagation perpendicular to strain, Fig. 3b). Figure 4 plots the theoretical penetration depth [Fig. 4a)] and plasmon propagation length [Fig. 4b)] against the excitation frequency or different directions of the applied strain and taking the plasmon propagation angle $\phi = 0$ at fixed value of the strain, $\varepsilon = 0.2$.

As can be seen, the penetration depth in the retarded approximation and the plasmon propagation length are maximum for plasmon propagation perpendicular to the direction of the applied strain. Hence, the penetration depth and the propagation length of surface plasmons can also be controlled by tunning the orientations of the applied strain in graphene.

3. Conclusions

The propagation of surface plasmons and penetration depth in graphene under uniform applied strain sandwiched by two isotropic dielectrics at THz frequencies have been investigated. We have shown that the penetration depth and the propagation length of surface plasmon depend on the magnitude and orientations of the applied strain with respect of the surface plasmon propagation in graphene. In a wide range of frequencies, the maximum propagation length and longer penetration depth are observed for perpendicular orientation. This opens new possibilities for controlling the propagation length and direction of surface plasmon propagation in graphene structures.

1. S. A. Maier, *Plasmonics: fundamentals and applications*, (Springer, 2007).
2. D. Fei, Y. Yuanqing, R. A. Deshpande and S. I. Bozhevolnyi, A review of gap-surface plasmon metasurfaces: fundamentals and applications, *Nanophotonics* **7** (2018) 1129-1156, https://doi.org/10.1515/nanoph-2017-0125.
3. X. Han, K. Liu and C. Sun, Plasmonics for biosensing, *Materials* **12** (2019) 1411, https://doi.org/10.3390/ma12091411.
4. V. G. Kravets *et al.*, Graphene-protected copper and silver plasmonics, *Sci. Rep.* **4** (2014) 5517, https://doi.org/10.1038/srep05517.
5. Xu Hailin, Wu Leiming, X. Dai, Y. Gao and Y. Xiang, An ultrahigh sensitivity surface plasmon resonance sensor based on graphene-aluminum-graphene sandwich-like structure, *Appl. Phys.* **120** (2016) 053101, https://doi.org/10.1063/1.4959982.
6. Y. Feng, Y. Liu and J. Teng, Design of an ultrasensitive SPR biosensor based on a graphene-MoS_2 hybrid structure with a MgF_2 prism, *Apl. Optics* **57** (2018) 3639, https://doi.org/10.1364/ao.57.003639.
7. P. O. Patil *et al.*, Graphene-based nanocomposites for sensitivity enhancement of surface plasmon resonance sensor for biological and chemical sensing: A review, *Biosens Bioelectron* **139** (2019) 111324, https://doi.org/10.1016/j.bios.2019.111324.
8. S. Huang, C. Song, G. Zhang and H. Yuan, Graphene plasmonics: physics and potential applications, *Nanophotonics* **6** (2017) 1191, https://doi.org/10.1515/nanoph-2016-0126.
9. W. Gong *et al.*, Experimental and theoretical investigation for surface plasmon resonance biosensor based on graphene/Au film/D-POF, *Op. Express* **27** (2019) 3483, https://doi.org/10.1364/OE.27.003483.
10. S. Chen and C. Lin, Figure of merit analysis of graphene-based surface plasmon resonance biosensor for visible and near infrared, *Op. Commun.* **435** (2019) 102, https://doi.org/10.1016/j.optcom.2018.11.031.
11. S. Chen and C. Lin, Sensitivity analysis of graphene multilayer based surface plasmon resonance biosensor in the ultraviolet, visible and infrared regions, *Appl. Phys. A* **125** (2019) 230, https://doi.org/10.1007/s00339-019-2515-y.
12. H. Vahed H. and C. Nadri, Ultra-sensitive surface plasmon resonance biosensor based on MoS_2-graphene hybrid nanostructure with silver metal layer, *Opt. Quantum Electronics* **51** (2019) 20, https://doi.org/10.1007/s11082-018-1739-y.
13. M. Sebek *et al.*, Hybrid plasmonics and two-dimensional materials: theory and applications, *J. Mol. Eng. Materials* **2** (2020) 20300001, https://doi.org/10.1142/S2251237320300016.
14. M. K. Alam *et al.*, Large graphene-induced shift of surface-plasmon resonances of gold films: effective-medium theory for atomically thin materials, *Phys. Rev. B* **2** (2020) 012008, https://doi.org/10.1103/PhysRevResearch.2.013008.
15. P. Yari, H. Farmani, A. Farmani, A. M. Mosavi, Monitoring biomaterials with light: review of surface plasmon resonance biosensing using two dimensional materials, *Preprints* (2021) 2021010483, https://doi.org/10.20944/preprints202101.0483.v1.
16. V. G. Kravets, F. Wu, T. Yu and A. N. Grigorenko, Metaldielectricgraphene hybrid heterostructures with enhanced sur-

face plasmon resonance sensitivity based on amplitude and phase measurements, *Plasmonics* **17** (2022) 973, https://doi.org/10.1007/s11468-022-01594-y.

17. J. Liu, S. Bao and X. Wang, Applications of graphene-based materials in sensors: a review, *Micromachines* **13** (2022) 184, https://doi.org/10.3390/mi13020184.
18. M. AlAloul and M. Rasras, Plasmon-enhanced graphene photodetector with CMOS-compatible titanium nitride, *J. Op. Soc. Am. B* **38** (2021) 602, https://doi.org/10.1364/JOSAB.416520.
19. L. Cui, J. Wang and M. Mengtao, Graphene plasmon for optoelectronics, *Rev. Phys.* **6** (2021) 100054, https://doi.org/10.1016/j.revip.2021.10005.
20. L. Tao *et al.*, Enhancing light-matter interaction in 2D materials by optical micro/nano architectures for high-performance optoelectronic devices, *InfoMat* **3** (2021) 36, https://doi.org/10.1002/inf2.12148.
21. M. Oliva-Leyva and G. Naumis, Understanding electron behavior in strained graphene as a reciprocal space distortion, *Phys. Rev. B.* **88** (2013) 085430, https://doi.org/10.1103/PhysRevB.88.085430; Effective Dirac Hamiltonian for anisotropic honeycomb lattices: optical properties, *Phys. Rev. B.* **93** (2016) 035439, https://doi.org/10.1103/PhysRevB.93.035439.
22. G. G. Naumis, S. Barraza-Lopez, M. Oliva-Leyva and H. Terrones, Electronic and optical properties of strained graphene and other strained 2D materials: a review, *Rep. Prog. Phys.* **80** (2017) 096501, https://doi.org/10.1088/1361-6633/aa74ef.
23. F. M. D. Pellegrino, G. G. N. Angilella and R. Pucci, Effect of uniaxial strain on plasmon excitations in graphene, *J. Phys. Conf. Ser.* **377** (2012) 012083, https://doi.org/10.1088/1742-6596/377/1/012083.
24. D. Dahal, G. Gumbs and D. Huang, Effect of strain on plasmons, screening, and energy loss in graphene/substrate contacts, *Phys. Rev. B* **98** (2018) 045427, https://doi.org/10.1103/PhysRevB.98.045427.
25. R. Hayn, T. Wei, V. M. Silkin and J. Van den Brink, Plasmons in anisotropic Dirac systems, *Phys. Rev. Mater.* **5** (2021) 024201, https://doi.org/10.1103/PhysRevMaterials.5.024201.
26. C. Lemus, G. Gonzalez de la Cruz, and M. Oliva-Leyva, Effect of uniform strain on graphene surface plasmon excitations, *Plasmonics* **18** (2023) 727, https://doi.org/10.21203/rs.3.rs-2410363/v1.
27. Z. Ma *et al.*, Directional control of propagating graphene plasmons by strain engineering, *Opt. Mater. Express* **12** (2022) 622, https://doi.org/10.1364/OME.447866.
28. N. D. Mermin, Lindhard dielectric function in the relaxation-time approximation, *Phys. Rev. B* **1** (1970) 2362, https://doi.org/10.1103/PhysRevB.1.2362.
29. M. Jablan, H. Buljan and M. Soljačić, Plasmonics in graphene at infra-red frequencies, *Phys. Rev. B* **80** (2009) 245435, https://doi.org/10.1103/PhysRevB.80.245435.
30. I.-T. Lin, Y.-P. Lai, K.-H. Wu, and J.-M. Liu, Terahertz optoelectronic property of graphene: substrate-induced effects on plasmonics characteristics, *Appl. Sci.* **4** (2014) 28, https://doi.org/10.3390/app4010028.